A. Saarenheimo, H. Talja*, and H. Keinänen†*

Fracture Mechanics Analysis of Destructive Large-Scale Pressure Vessel Tests

REFERENCE Saarenheimo, A., Talja, H., and Keinänen, H., **Fracture mechanics analysis of destructive large-scale pressure vessel tests**, *Defect Assessment in Components – Fundamentals and Applications*, ESIS/EGF9 (Edited by J. G. Blauel and K.-H. Schwalbe) 1991, Mechanical Engineering Publications, London, pp. 957–973.

ABSTRACT Within the Nordic countries a four-year research programme in elastic–plastic fracture mechanics was initiated in 1985. The main technical objective of the programme was to verify the leak before break concept. In this paper the results of analytical and numerical simulations for two destructive tests with large scale pressure vessels are presented. To verify numerical and analytical assessments two tests were performed with a large size pressure vessel which was pressurised by water up to rupture. The vessel had dimensions comparable to nuclear reactor pressure vessel. For both tests an artificial sharp surface flaw was made on the inner wall of the vessel.

In the first experiment the surface flaw was long and rather shallow. According to engineering assessment methods a catastrophic failure was expected. However, one of the circumferential welds in the vessel intersected the flaw at the middle of its length and the failure occurred as a local leak in the rather brittle weld area. Some crack growth occurred along the whole crack front. Detailed post-test calculations using three-dimensional elastic–plastic finite element models were carried out. The fracture behaviour could be described with these analyses.

For the second test the vessel was repaired. A shorter and deeper flaw was produced in the repair block, purely in base material. Engineering methods estimated the situation to be a leak before break. In the second test the flaw penetrated the wall along its whole front but did not extend axially. Thus the fracture behaviour was correctly assessed but the estimated failure pressures were quite conservative. The main reason for the conservativeness was probably the residual stresses due to the repair welding. To assess this effect two-dimensional FE analyses were performed.

Introduction

Safety and integrity assessments of pressure vessels can always be performed using complete three-dimensional finite element analysis but the costs may become unacceptably high. Therefore different engineering analysis methods are used. Examples of such methods are R6 **(1)(2)** and other failure assessment diagram (FAD) methods and Battelle's method **(3)**. The accuracy and validity of the engineering methods are most appropriately evaluated by comparing calculated results with those from experiments. Realistic computational fracture analysis, on the other hand, necessitates reliable determination and application of relevant material property parameters.

* Technical Research Centre of Finland (VTT), Nuclear Engineering Laboratory, PO Box 169, SF-00181 Helsinki, Finland.
† Technical Research Centre of Finland (VTT), Metals Laboratory, PO Box 26, SF-02151 Espoo, Finland.

Within an extensive Nordic research programme in elastic–plastic fracture mechanics, the main technical objective was to verify the leak-before-break concept. To validate numerical and analytical evaluations two tests were made pressurising a large size pressure vessel by water up to rupture. For both tests an artificial sharp surface flaw was made on the inner wall of the vessel. In this paper the results of analytical and numerical simulations for the two destructive tests are presented and compared with experimental findings.

Experimental study

Test geometry

The tests were carried out on a large decommissioned pressure vessel (shown in Fig. 1) which had been used as a hydrogen cracking reactor in Neste Oy's oil refinery plant from 1965 **(4)(5)**. The design pressure and temperature were 144 bar and 471°C. The vessel was fabricated of hot-formed rings with axial weldments and two hot-formed heads. The rings were welded together with circumferential weldments. The pressure vessel material was a heat resistant high strength steel 2.25 percent Cr 1 percent Mo. The wall thickness of the

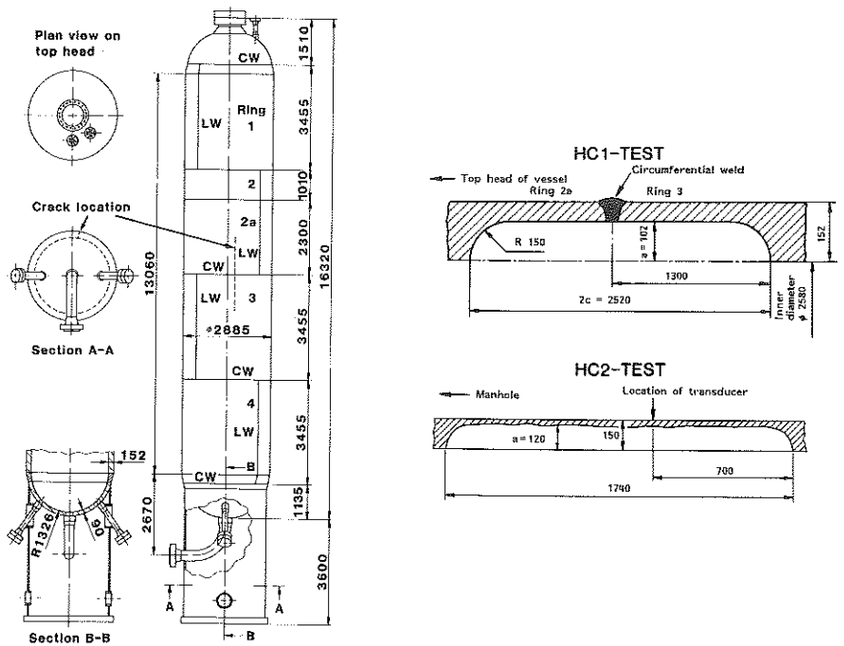

Fig 1 Decommissioned HC reactor pressure vessel of an oil refinery plant and dimensions of the axial surface flaw produced into the pressure vessel. CW, circumferential weldment; LW, longitudinal weldment

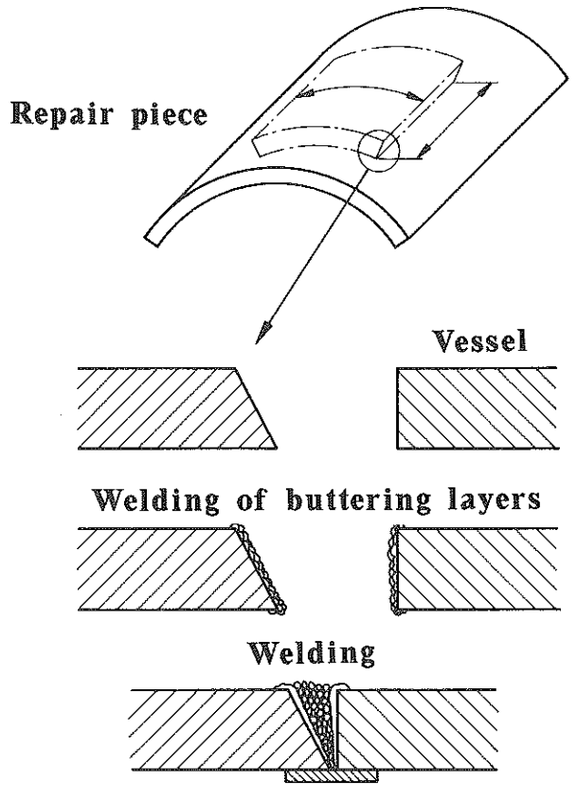

Fig 2 Repair welding procedure of the HC pressure vessel after the HC1 test with a repair piece removed from an identical sister vessel. Before welding an artificial axial flaw was produced into the repair piece

rings and heads was without cladding 152 mm and 60 mm, respectively. The inside wall of the vessel was clad with a 7 mm thick stainless steel layer which was partly separated from the base metal during the operation.

The strength properties of base and weld materials were not very different but the crack growth resistance curves differed drastically as will be shown further on (Fig. 7). According to the stress strain measurements for the first test, the flow stress (calculated as the average of the yield and ultimate stresses) for base material was 379 MPa and for weld material 438 MPa.

For the first test, an artificial, sharp axial flaw was introduced into the inner wall of the vessel. The flaw was prepared by applying a special grinding and welding technique. One of the circumferential welds in the vessel intersected the flaw at the middle of its length. The second test was performed with the same pressure vessel as the first test. The vessel was repaired by welding a repair piece from a sister vessel applying temper bead technique. The new flaw located purely in base material in the repair piece. The dimensions of the

vessel and the flaws are given in Fig. 1 and the repair welding procedure is depicted in Fig. 2.

Test instrumentation

For the tests the vessel was extensively instrumented to record the events during testing so that membrane stresses, crack mouth opening displacement CMOD, vessel ovalisation, crack initiation and growth, pressure, and temperature could be determined. The failure behaviour was monitored with strain gauges, DC potential drop technique (only in the first test) and acoustic emission measurements. The potential difference across the crack, near the crack faces, as well as CMOD were measured at three positions: at the half way, at a quarter of the crack length, and near the crack end. The acoustic emission (AE) instrumentation of the pressure vessel was planned so as to monitor the entire vessel, as in normal hydrotest, and also to more precisely monitor the defect area.

Failure behaviour

In the first test an acoustic noise was heard when the pressure was increased to 130 bar. It indicated presumably a pop-in because no leak was detected. Simultaneously, a sudden discontinuity was seen in the CMOD versus pressure curve (Fig. 3). When a pressure value of 170 bar was reached, a narrow local leak occurred in the circumferential weld. After this the pressure could be increased up to 186 bar. Then the leak rate became equal to the capacity of the pumps and the test was interrupted.

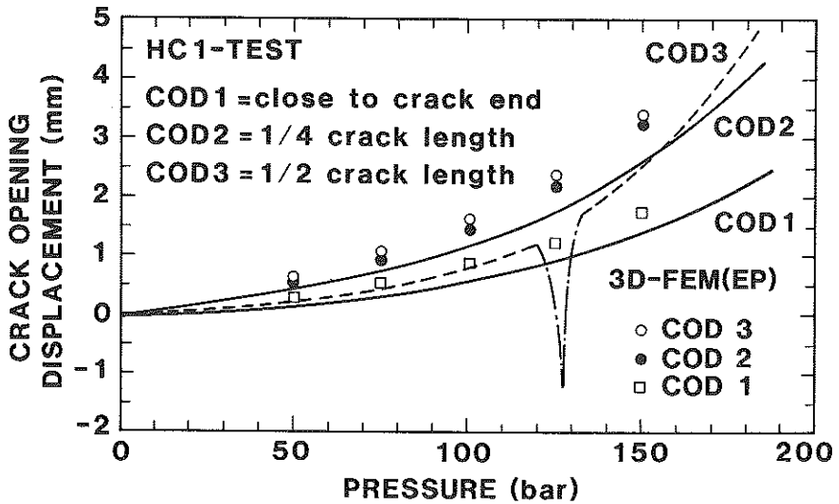

Fig 3 Crack opening displacement measurements at three sites of the crack length

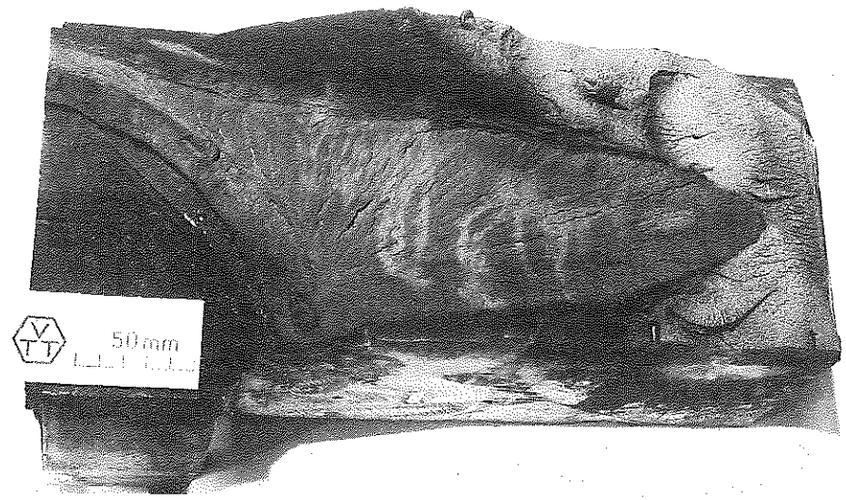

Fig 4 Shape of the crack end after HC2 test

In the second test the crack growth initiated in the pressure range of 120–130 bar. The flaw penetrated the wall simultaneously almost along its whole length at the pressure value of 189 bar. No crack growth occurred in axial direction except for a local pop-in type extension at the circular part of the crack front (Fig. 4) and thus the failure remained as leak.

Calculational assessments

Assessments for the first test (HC1-test)

Engineering assessment methods were used for pre-test calculations. The aim of the calculations was to choose suitable flaw dimensions and to estimate the leak-before-break condition in the test. After the test extensive best estimate analyses were performed using three-dimensional elastic–plastic finite element models.

Engineering analyses for the HC1-test

Pre-calculations were performed using the Batelle's (3) method and R6-method (1)(2). As a result of the calculations made using the Battelle's method, a flaw with the length of 1.6 m and the depth of 110 mm was recommended. Due to fabrication problems, however, a crack deeper than 100 mm was not possible. To keep the burst pressure below about 200 bar a flaw with the length of 2.5 m and the depth of 100 mm was produced. The estimates for the critical pressure results are summarised in Fig. 5.

The unstable crack extension in the length direction after ligament rupture was also estimated analytically. The crack length at which the stress intensity

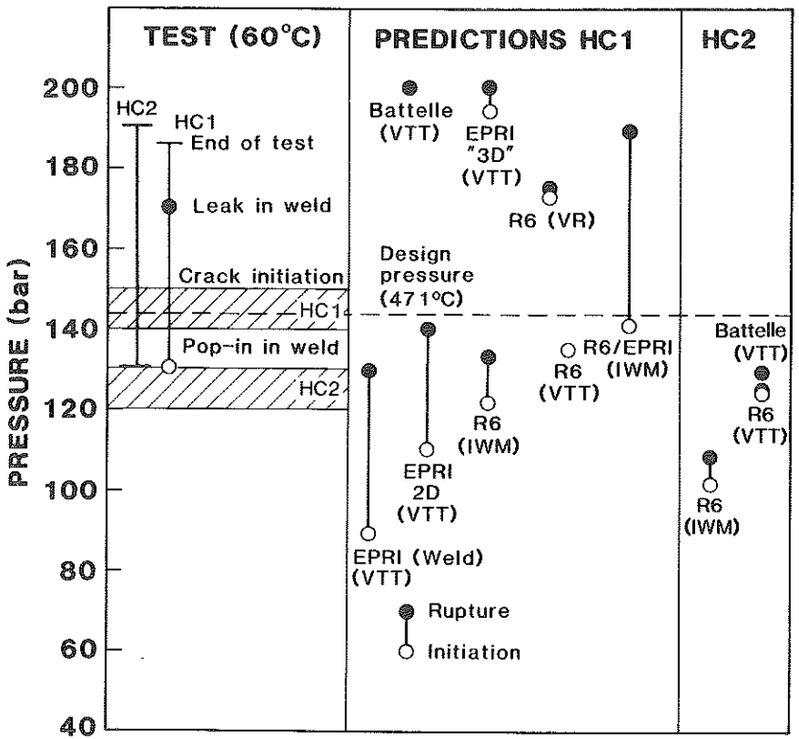

Fig 5 Summary of the results for pre-test analyses for the HC1 and HC2 tests

factor value is equal to the arrest value was estimated by taking into account the pressure drop in the vessel and the enlargement of the leak area. Those investigations predicted axial crack extension from three to six metres. Pre-test calculations to assess the critical pressure value were performed by Veritas Research (VR, Norway), Fraunhofer-Institut für Werkstoffmechanik (Fh-IWM, Federal Republic of Germany) and Technical Research Centre of Finland.

Finite element analyses for the HC1-test

As the post-test calculations for the HC1-test, extensive three-dimensional elastic–plastic finite element analyses were performed (4). In the calculations the effect of the brittle weld intersecting the flaw and the effect of the maintenance deck, which was not totally removed before the test, were considered. The finite element analyses were carried out using the ADINA-code (6) and the J integral values were calculated using the post-processor programme VTTVIRT.

Figure 6 shows the finite element mesh used in the calculations. Because of two symmetry planes, only one quarter of the pressure vessel had to be model-

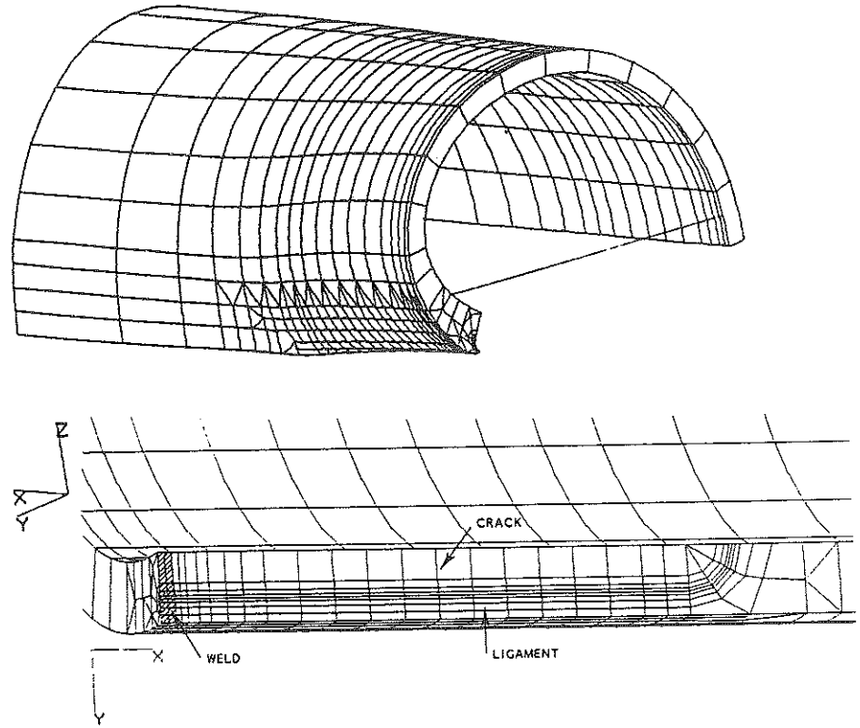

Fig 6 Finite element model used for the three-dimensional fracture assessment of the HC1 test

led. The axial length of the model was limited to 3.5 m. There were 1100 15- and 20-noded volume elements and over 16 000 degrees of freedom. One beam element was needed to simulate the effect of the maintenance deck. To model the crack front area collapsed elements causing a $1/r$ singularity in the strains near the crack front were adopted. Hence the cladding was not thought to influence the fracture behaviour of the vessel. Different material properties of the base and the weld materials were taken into consideration applying multi-linear stress strain curves. The von Mises yield function with isotropic yield hardening was adopted. The geometric non-linearities were considered using the updated Lagrangian formulation.

Two different analyses with stationary cracks were carried out. The aim of the first one with the original surface crack geometry was to find out where the crack starts to grow and to estimate the amount of the stable crack growth along the artificial crack front. The aim of the second analysis with the through-the-wall-crack geometry was to study whether a narrow through-the-wall crack in the surface crack ligament tends to grow in the axial direction, i.e., into the base metal. As the final result the crack shape at the end of the

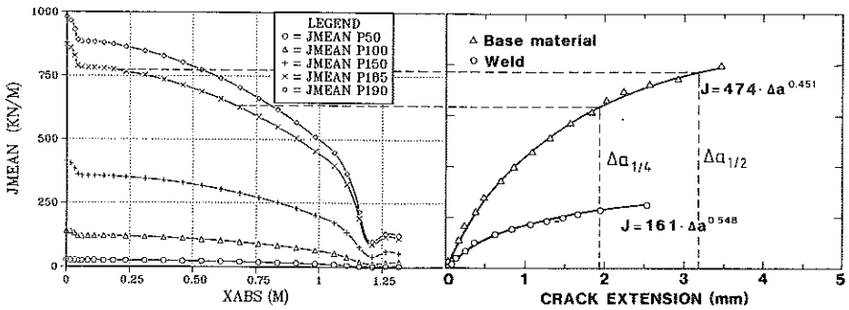

Fig 7 ***J*** **integral variations along the original flaw in the HC1 test at different pressure levels (bar) with crack growth resistance curves for base and weld metals, measured from 25 CT specimens with 20 percent side grooving**

test was assessed. The assessment was based on the calculated J integral variations along the original flaw front (Fig. 7) and along a narrow through-the-wall crack having the same width as the actual leak in the circumferential weld (Fig. 8) area together with measured crack growth resistance curves. In calculating J values, the pressure along the crack faces was taken into consideration. The estimated and measured crack shapes are compared in Fig. 9.

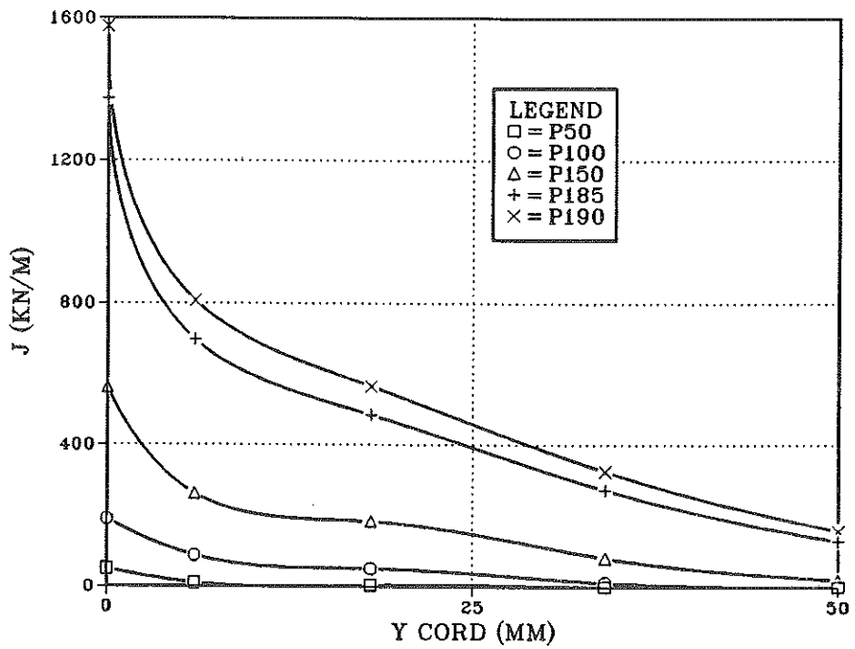

Fig 8 ***J*** **integral variations along the narrow through-the-wall crack in the HC1 test at different pressure values (bar,** $y = 0$ **at the original artificial flaw front and** $y = 50$ **at the outer surface)**

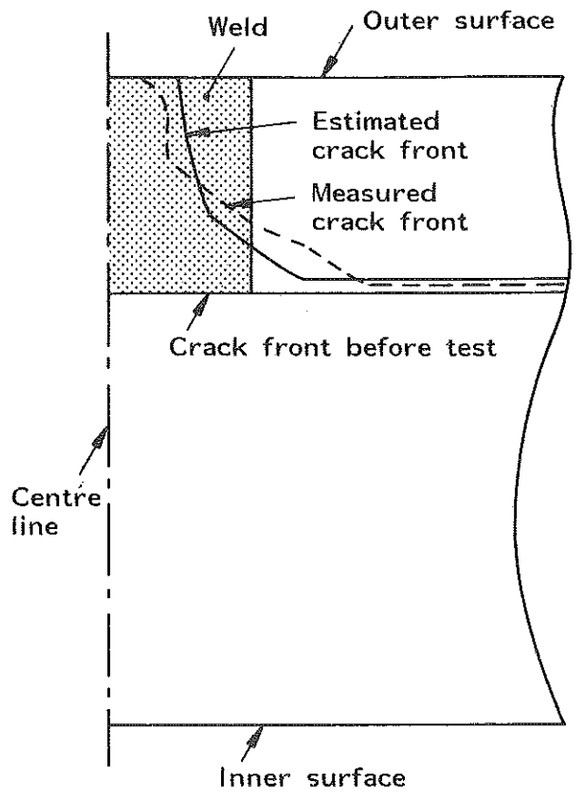

Fig 9 Estimated and measured crack shape after the HC1 test

Assessments for the second test (HC2-test)

The assessments for the second pressure vessel test comprised engineering analyses to choose the flaw dimensions, assess the failure load and two-dimensional finite element analyses to estimate the effect of the welding residual stresses (5).

Engineering analyses for the HC2-test

Before the test, engineering assessments were made by Fh-IWM and VTT. The results are summarised in Fig. 5. On the basis of Battelle's limit load method the estimated failure pressure was 130 bar. R6-method estimates by Fh-IWM and VTT were 108 and 125 bar. The residual stresses tended to close the crack so that CMOD was −0.8 mm after welding. One can think that the failure is caused by the pressure exceeding the value (60 bar) at which CMOD was 0.8 mm. In this way estimates quite close to the experimental value (189 bar) are obtained.

Additional investigations were made with the R6-method to estimate the sensitivity of the assessment when different parameters were varied. Revisions 2 and 3 of the method were used and in the case of revision 3 options 1 and 2 were applied. At first the failure estimation was repeated with mean material parameter values (σ_y = 329 MPa, σ_u = 522 MPa, J_{IC} = 275 N/mm, C = 437.5 and n = 0.5) and actual crack depth using revisions 2 and 3 (options 1 and 2) of the R6 method. The results are summarised in Table 1. Largest failure load estimate was obtained according to revision 2 though this revision does not consider the strain hardening of the material. This is due to the fact that the failure mode is nearly a pure collapse of the ligament. In revision 2 the collapse load estimate is based on the flow stress and in revision 3 the coordinate axis value is defined using the yield load. Thus, in the present analysis with the revision 2, the horizontal coordinates correspond to the limit load estimation purely with the Battelle method.

In the next stage a series of calculations was made varying the material parameter values, crack depth and the Ramberg–Osgood fit of the material law. Except for the Ramberg–Osgood fit which was studied with the revision 3 option 2, the calculations were made using the revision 2. The flow stress varied between 418 and 435 MPa and J_{Ic} was in the range of 200 to 350 N/mm. In the exponential function presentation of the crack growth resistance curve, the factor C varied between 375 and 500. The exponent n was kept as 0.5. The minimum J_{IC} was used simultaneously with the minimum C-value and the maximum values were used respectively. The crack depth was varied by adding and subtracting 2 mm from the actual value. The results are given in Table 1. At each calculation only one parameter is different than in the solution with mean parameter values. Figure 10 shows the results when the flow stress and the crack growth resistance curve are varied. The assessment points are defined at the pressure value of 10 MPa. Figure 11 shows three

Table 1 Summary of the results of the sensitivity analysis with the R6-method

	Initiation pressure (bar)	*da (mm)*	*Instability pressure (bar)*
Mean Rev. 2	137	0.5	140
Mean Rev. 3 option 1	116	0.5	117
Mean Rev. 3 option 2	121	0.5	122
a_{min}	143	0.5	147
a_{max}	129	0.5	131
$\sigma_{f\,min}$	135	0.4	138
$\sigma_{f\,max}$	139	0.4	143
$J_{R\,min}$	128	0.7	137
$J_{R\,max}$	139	0.2	140
R–O$_{min}$	115	0.8	118
R–O$_{mean}$	116	0.9	120
R–O$_{max}$	117	1.4	124

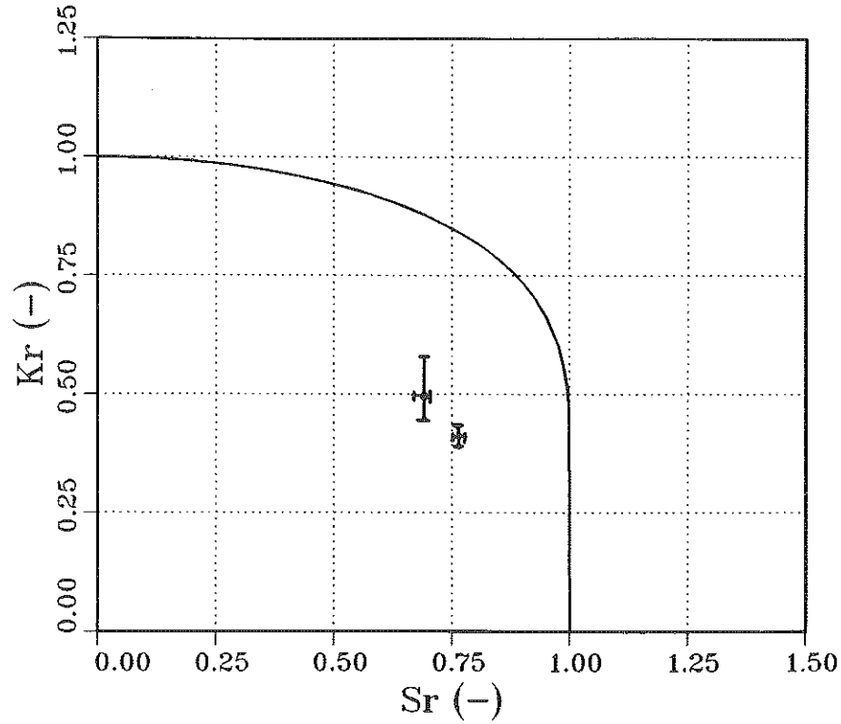

Fig 10 Sensitivity of R6 estimates when flow stress and crack growth resistance are varied – upper left: initiation and lower right: instability

different Ramberg–Osgood fits for the measured stress strain curve. The results based on the lower, mean, and upper fit are compared in Table 1.

Numerical simulation of welding procedure

In the second test the residual stresses due to the repair welding seemed to affect the fracture behaviour. Therefore it was decided to study at first with relatively simple models, how those stresses could be appropriately considered in detailed post-test analyses. Extensive best estimate analyses are not meaningful before the boundary conditions can be reasonably modelled.

Butt-welding of plates. So far, numerical simulation of welding procedures has been applied only to very simple geometries using two-dimensional models. As an example, temperature and stress fields in a submerged arc welded plates were calculated. This case has also been analysed by Andersson (7). The structure is shown in Fig. 12. Two plates are joined together with a single weld deposit from the upper part. The complicated thermomechanical problem was solved with a two-dimensional finite element model (Fig. 12) using the ADINA code.

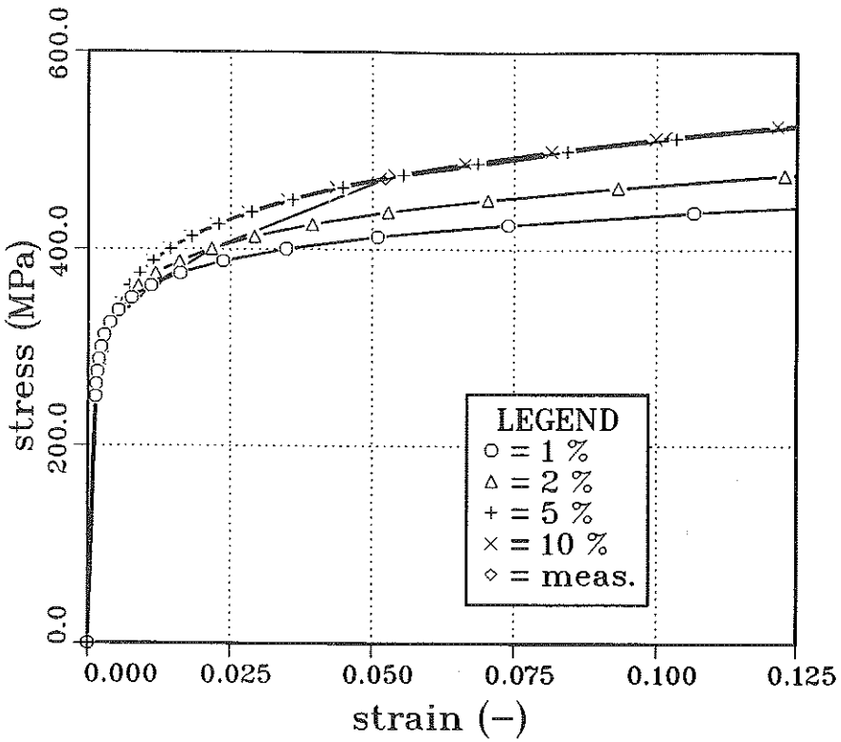

Fig 11 Different Ramberg–Osgood fits for the pressure vessel material

The coupling effect between the temperature and stress field was assumed to be small. Therefore, the thermal and mechanical analyses were carried out separately. The thermoelastic–plastic material model of ADINA without creep and hardening was used. Phase transformations were taken into account at certain temperature intervals by modifying the material parameters. Calculated results correlated well with Andersson's experimental and numerical data, Fig. 13. Contours of the calculated residual stress component σ_x are shown in Fig. 14. The temperature field was also calculated with a three-dimensional model. Although the size of the model was reduced, the solution time became impractically large.

As regards to the residual stress distribution in the HC2 test vessel, still many questions remain open. The application of this kind of numerical analysis technique to a complicated three-dimensional multipass welding problem (as the repair welding of the HC2 vessel is) does not seem to be possible at this stage. Therefore a very simple method was used to assess the effect of welding, as is described in the following.

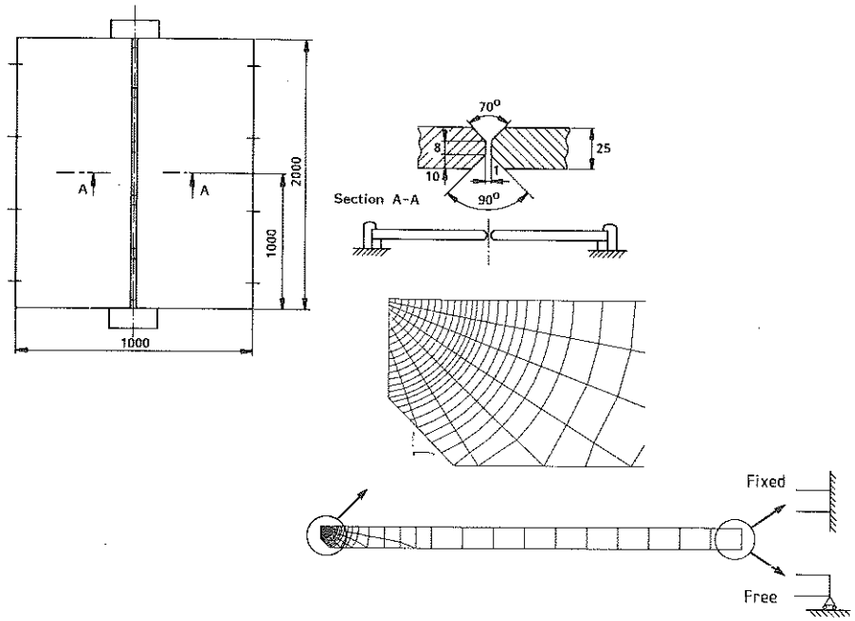

Fig 12 The welded plate structure and the finite element model

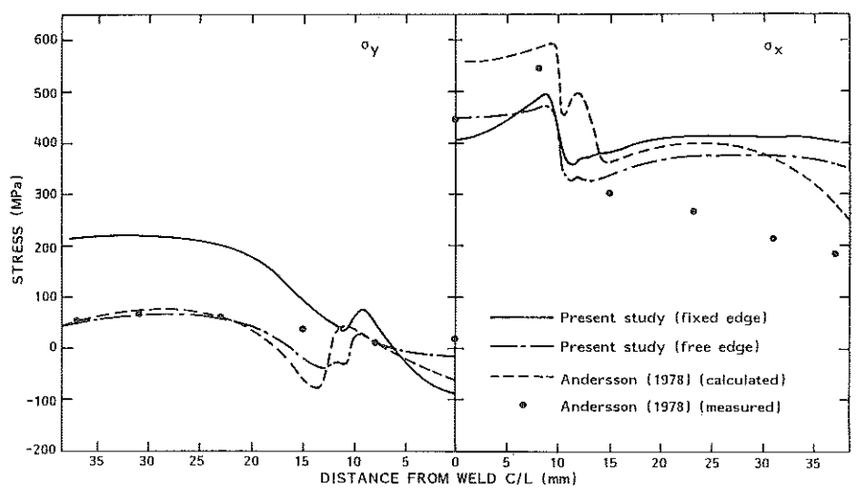

Fig 13 Stress distribution after butt-welding of plates

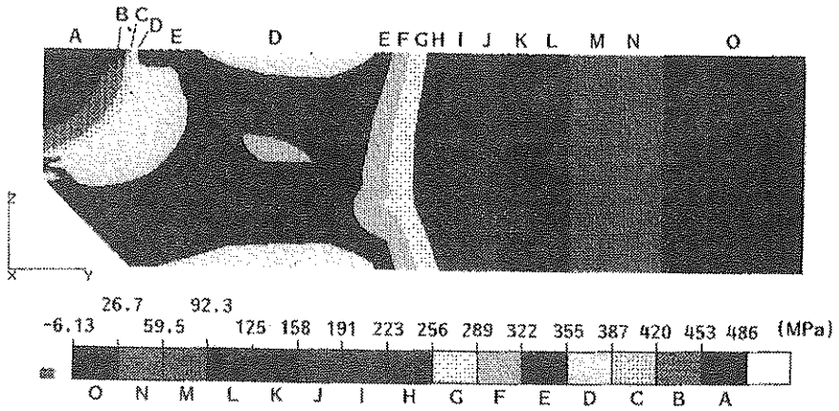

Fig 14 Contours of the residual stress component σ_x (free edge case)

Repair welding of tested pressure vessel. Two-dimensional finite element analyses were carried out in order to simulate roughly the behaviour of the pressure vessel due to possible welding residual stresses in the HC2 test. First the behaviour in pure pressure loading was studied, without taking the effect of the welding into consideration, and compared with experimental findings. The measured and calculated diameter changes are compared in Fig. 15 as a

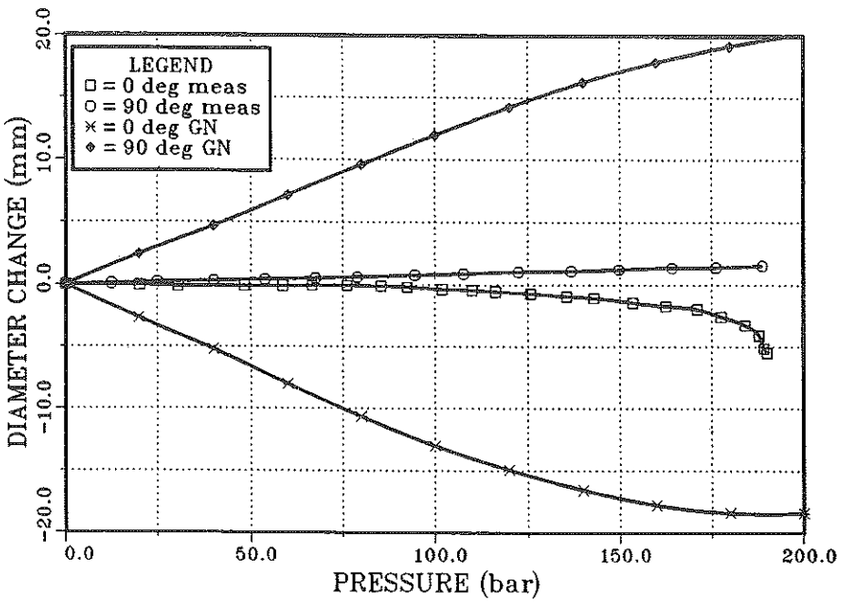

Fig 15 Measured and calculated diameter changes due to pressure loading

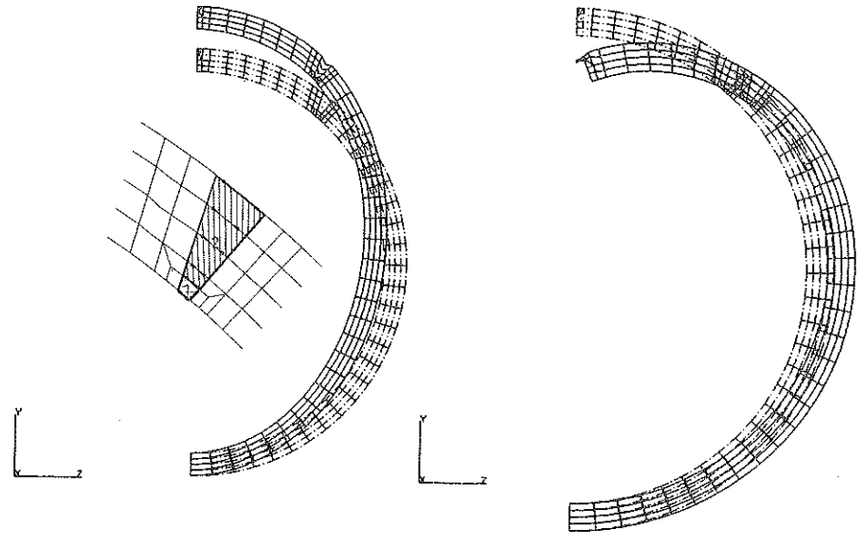

Fig 16 Description of welding and deformed finite element meshes (a) due to welding and (b) due to pure pressure loading

function of pressure. Two-dimensional results are often very conservative but in this case even the overall behaviour was quite different. According to the calculation the flaw deflects to the inside of the vessel (Fig. 16(b)), but the measured diameter change remains nearly zero in the crack location until the pressure reaches the value of 80 bar. Also the measured and the calculated strain values along the vessel circumference did not agree at all.

The second calculation was made with the same model as the first one. The welding was modelled with linearly distributed loads which simulate the shrinkage of the weld material (Fig. 16(a)). The loads were chosen so that the crack mouth opening value corresponded to the measured value during the welding process (9). The calculation was made in two steps. At the first step one element layer was added into the model to describe the weld. A face load was applied along the element edge. The CMOD value was 0.2 mm after the first atep. In the second step the rest of the elements simulating the welding and face loads at their edges were added. At the end of the second step, the CMOD was −0.8 mm. The deformed shape of the model is shown in Fig. 16(a). The calculated hoop stress distribution after the welding corresponded reasonably to the measured one and the diameter change corresponded to the measured initial shape of the vessel.

Summary and conclusions

The test programme comprised of two tests with a large pressure vessel. In the pre-test and post-test analyses engineering methods and the finite element

method were adopted. The engineering methods used were Battelle's limit load method and the R6 method. The finite element analyses consisted of two- and three-dimensional linear, materially and geometrically non-linear analyses.

If the material is ductile, and the geometry and loading are simple, i.e., cylindrical geometry, homogeneous material properties, and axial or circumferential crack orientation, then Battelle's limit load method gives the bursting load and the stability of the burst crack with low costs and a quite reasonable accuracy. One of the biggest problems is how to choose the flow stress for the calculations. The R6 method is useful because it can be used to estimate stable crack growth before bursting. It can be also used to determine the most probable failure mode if the material is not fully ductile. One more advantage is that sensitivity analyses varying geometrical dimensions and material parameter values can be effectively made.

In case of a realistic infinitely long flaw even in a simple structure, as in a cylindrical pressure vessel, three-dimensional effects are essential and three-dimensional finite element calculations are necessary to estimate the behaviour accurately. This is usually rather expensive but gives very detailed informtion, e.g., stresses and strains at every interesting point and J integral distributions along crack front at different load levels. The amount of stable crack growth and the fracture behaviour can be assessed based on the calculated J variations and the measured J_R curves. In real component assessments the situation does not generally correspond to an 'ideal case'. A more complicated behaviour may be caused by a complicated geometry, combined loading or multiple materials as in cladded pressure vessels or weldments. Extensive three-dimensional finite element analyses may be then the only way to explain the failure behaviour. The proper consideration of boundary conditions and availability of the relevant material parameter data are very essential for achieving good results.

As regards to the present cases, the experimental results deviated clearly from the engineering assessments. In connection to the first test it could be explained with geometrical effects which were considered in finite element calculations. Calculated changes of the diameter, COD, and strain values based on three-dimensional analysis showed a good agreement with the measured ones (4). In the case of the second test the repair welding residual stresses affected the failure behaviour. So far this effect has been explained only qualitatively. Further investigations are needed before extensive post-test analyses can be made.

Acknowledgement

This work was funded by the Nordic Council of Ministers, Technology Development Centre (TEKES), Finnish Centre for Radiation and Nuclear Safety (STUK), Ministry for Trade and Industry in Finland (KTM), Swedish Nuclear Power Inspectorate (SKI), Neste Oy, Imatra Power Co. (IVO), Helsinki Energy Board (HKE) and Technical Research Centre of Finland.

References

(1) HARRISON, R. P., LOOSEMORE, K., MILNE, I., and DOWLING, A. R. (1980) Assessment of the integrity of structures containing defects, CEGB Report R/H/R6-Rev. 2.
(2) MILNE, I., AINSWORTH, R. A., DOWLING, A. R., and STEWART, A. T. (1988) Assessment of the integrity of structures containing defects, *Int. J. Pressure Vessels Piping*, **32**, 3–104.
(3) RODABAUGH, E. C. (1985) Comments on the leak-before-break concept for nuclear power plant piping systems, Oak Ridge National Laboratories, NUREG/CR-4305.
(4) SAARENHEIMO, A., TALJA, H., IKONEN, K., RINTAMAA, R., KEINÄNEN, H., and TÖRRÖNEN, K. (1990) Fracture behaviour simulation of a flawed full-scale pressure vessel, *Int. J. Pressure Vessels Piping*, **41**, 75–101.
(5) RINTAMAA, R., TALJA, H., SAARENHEIMO, A., KEINÄNEN, H., WALLIN, K., and IKONEN, K. (1989) Validation of experimental and computational fracture assessment methods for flawed pressure components, Paper presented at the SMiRT-10 Post Conference Seminar no 2. Monterey, CA.
(6) BATHE, K. H. (1980) ADINA, A finite element program for automatic dynamic incremental nonlinear analysis, Report 82 448-1, MIT, Cambridge MA.
(7) ANDERSSON, B. A. B. (1978) Thermal stresses in a submerged-arc-welding joint considering phase transformations, *J. Engng Mater. Technol.*, **100**, 356–362.